Available online at www.sciencedirect.com
SCIENCE DIRECT®
Journal of Sound and Vibration 289 (2006) 987–998
JOURNAL OF SOUND AND VIBRATION
www.elsevier.com/locate/jsvi

Dynamics of vibrating systems with tuned liquid column dampers and limited power supply

S.L.T. de Souza[a], I.L. Caldas[a], R.L. Viana[b,*], J.M. Balthazar[c], R.M.L.R.F. Brasil[d]

[a]*Instituto de Fisica, Universidade de São Paulo, C.P. 66318, 05315-970, São Paulo, SP, Brazil*
[b]*Departamento de Fisica, Universidade Federal do Paraná, C.P. 19081, 81531-990, Curitiba, Paraná, Brazil*
[c]*Departamento de Estatistica, Matemática Aplicada e Computacional, Instituto de Geociências e Ciências Exatas, Universidade Estadual Paulista, C.P. 178, 13500-230, Rio Claro, SP, Brazil*
[d]*Departamento de Engenharia Estrutural e de Fundações, Escola Politécnica, Universidade de São Paulo, 05424-930, São Paulo, SP, Brazil*

Received 6 July 2004; received in revised form 25 February 2005; accepted 2 March 2005
Available online 31 May 2005

Abstract

Tuned liquid column dampers are U-tubes filled with some liquid, acting as an active vibration damper in structures of engineering interest like buildings and bridges. We study the effect of a tuned liquid column damper in a vibrating system consisting of a cart which vibrates under driving by a source with limited power supply (non-ideal excitation). The effect of a liquid damper is studied in some dynamical regimes characterized by coexistence of both periodic and chaotic motion.

1. Introduction

The need of mitigate wind, ocean wave and earthquake-induced vibrations in structures like tall buildings, long span bridges and offshore platforms has led to a steadfast interest

*Corresponding author.
E-mail address: viana@fisica.ufpr.br (R.L. Viana).

0022-460X/$ - see front matter © 2005 Elsevier Ltd. All rights reserved.
doi:10.1016/j.jsv.2005.03.001

in damping devices. Impact dampers are a very useful way to suppress unwanted high-amplitude vibrations in small-scale systems, but they are somewhat difficult, if not impossible, to implement in large-scale engineering structures [1,2]. For the latter systems the tuned liquid dampers (TLDs) and tuned liquid column dampers (TLCDs) have gained a special attention by virtue of their simplicity and flexibility [3]. A tuned liquid damper is basically a mass-spring-dash-pot system connected to the structure, and works due to the inertial secondary system principle, by which the damper counteracts the forces producing the vibration [4].

A TLCD replaces the mass-spring-dash-pot system by a U-tube-like container where the motion of a liquid column absorbs part of the vibration on the system, with a valve/orifice playing the role of damping. An TLCD has the additional advantage of being a low-cost application. In a tall building, for example, the container can also be used as a building water supply, whereas in an TLD the mass-spring-dash-pot is a dead-weight component without further use [5]. In fact, vibration control through TLCD has been recently used in other engineering applications, such as ship and satellite stabilization.

Whereas the damping of a mass-spring-dash-pot system characteristic of a TLD is essentially linear, the damping in a liquid column is amplitude-dependent (regulated by the orifice in the bottom of the U-tube) and consequently nonlinear. Hence, the dynamics of a TLCD is far from being simple, and very few analytical results can be obtained. Numerical explorations of the dynamics of a TLCD mounted on a structural frame, using a non-ideal motor as a source of energy, have been performed recently [3].

Non-ideal motors are forcing sources with limited energy supply, in such a way that their behavior also depends on the vibrating system [6]. In fact, the forcing becomes an active part of the dynamics, and this leads to systems with more degrees of freedom, and more equations of motions are thus needed to describe the problem [7]. We must borne in mind that, in practice, every driving source has a limited power supply, and ideal motors are actually an idealization. Impact dampers, using particles bouncing back and forth, and subjected to non-ideal forcing have been recently studied from the point of view of complex dynamics, presenting regular and chaotic motion for wide parameter intervals [8–10].

In this paper we study the dynamics of a vibrating system consisting of a moving cart attached to a spring–dash–pot under non-ideal (limited power supply) motor, and endowed with a TLCD. The combination of nonlinear damping of the liquid column, the spring nonlinearity and the non-ideal nature of the forcing makes for a rich dynamical behavior which we investigate numerically. The main motivation underlying our investigation is the fact that amplitude damping of vibrations cannot be taken for granted if a TLCD is mounted on a structure driven by a limited power supply source. In fact, there are situations in which the damping effectiveness of TLCD is very low, and even complex motion may appear, such as large-amplitude chaotic motion, which can be highly undesirable. It is of paramount importance to analyze the parameter intervals for which damping due a TLCD can be effective, and this is the key point to be treated in this paper.

This paper is structured as follows: in Section 2 we describe the model equations for the cart endowed with a TLCD under non-ideal forcing. Section 3 explores some aspects of the model dynamics, emphasizing the role of forcing parameters on the effectiveness of vibration damping and/or amplification.

2. Theoretical model

In the following we will consider the 1D motion of a cart of mass M connected to a fixed frame by a nonlinear spring and a dash-pot (viscous coefficient c) (Fig. 1). The nonlinear spring force is given by $k_1X - k_2X^3$, where X denotes the cart displacement with respect to some equilibrium position in the absolute reference frame. The motion of the cart is due to an in-board non-ideal motor with moment of inertia J and driving an unbalanced rotor. We denote by φ the angular displacement of the rotor, and model it as a particle of mass m_0 attached to a massless rod of radius r with respect to the rotation axis. Here $\tilde{E}_1$ and $\tilde{E}_2$ are damping coefficients for the rotor, which can be estimated from the characteristic curve of the energy source (a DC-motor) [8].

The TLCD consists of a U-tube attached to the top of the moving cart, containing a liquid of total mass m and density ρ. The cross-sectional area of the tube is A, and with a distance b between the two vertical columns. The distance between the liquid levels in these columns will be denoted ℓ and is obviously a constant. The vertical displacement of the left column with respect to the liquid level when the cart is in rest is denoted Y. There is a valve at the middle point of the bottom of the TLCD whose aperture can be tuned in order to vary the resistance to the flow through this orifice. This is the source of the nonlinear and amplitude-dependent damping experienced by the liquid mass while flowing through the U-tube. The coefficient of head loss of the valve is ξ.

The motion of the combined cart-liquid damper system is governed by the following equations [3]:

$$(M+m)\frac{\mathrm{d}^2X}{\mathrm{d}t^2} + c\frac{\mathrm{d}X}{\mathrm{d}t} - k_1X + k_2X^3 = m_0r\left[\frac{\mathrm{d}^2\varphi}{\mathrm{d}t^2}\sin\varphi + \left(\frac{\mathrm{d}\varphi}{\mathrm{d}t}\right)^2\cos\varphi\right] - \alpha m\frac{\mathrm{d}^2Y}{\mathrm{d}t^2}, \tag{1}$$

$$(J+m_0r^2)\frac{\mathrm{d}^2\varphi}{\mathrm{d}t^2} = m_0r\frac{\mathrm{d}^2X}{\mathrm{d}t^2}\sin\varphi + m_0rg\cos\varphi + \tilde{E}_1 - \tilde{E}_2\frac{\mathrm{d}\varphi}{\mathrm{d}t}, \tag{2}$$

$$m\frac{\mathrm{d}^2Y}{\mathrm{d}t^2} + \frac{m\xi}{2\ell}\left|\frac{\mathrm{d}Y}{\mathrm{d}t}\right|\frac{\mathrm{d}Y}{\mathrm{d}t} + k_3Y = -\alpha m\frac{\mathrm{d}^2X}{\mathrm{d}t^2}, \tag{3}$$

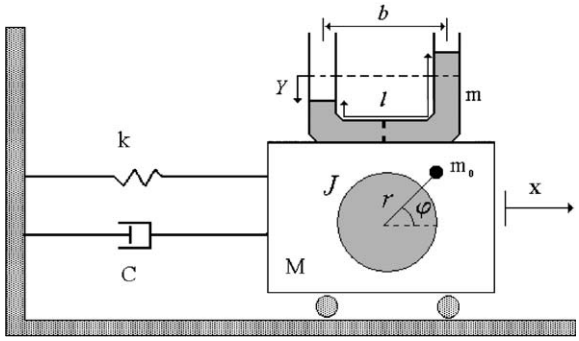

Fig. 1. Schematic model of a cart oscillation driven by a rotor and with a tuned liquid column damper.

where g is the gravity acceleration, $\alpha = b/\ell$ is the length ratio of the U-tube, and k_3 the effective (linear) stiffness of the liquid column, as it undergoes oscillations inside the TLCD.

It is convenient to work with dimensionless positions and time, according to

$$X \to x \equiv \frac{X}{r}, \tag{4}$$

$$Y \to y \equiv \frac{Y}{r}, \tag{5}$$

$$t \to \tau \equiv t\sqrt{\frac{k_1}{M}} \tag{6}$$

in such a way that Eqs. (1)–(3) are rewritten in the following form:

$$(1+\mu)\ddot{x} + \beta\dot{x} - x + \delta x^3 = \varepsilon_1(\ddot{\varphi}\sin\varphi + \dot{\varphi}^2\cos\varphi) - \alpha\mu\ddot{y}, \tag{7}$$

$$\ddot{\varphi} = \varepsilon_2\ddot{x}\sin\varphi + \varepsilon_3\cos\varphi + E_1 - E_2\dot{\varphi}, \tag{8}$$

$$\ddot{y} + \gamma|\dot{y}|\dot{y} + \sigma y = \alpha\ddot{x}, \tag{9}$$

where the dots stand for differentiation with respect to the scaled time τ, and the following abbreviations were introduced:

$$\mu \equiv \frac{m}{M}, \quad \beta \equiv \frac{c}{\sqrt{k_1 M}}, \quad \delta \equiv \frac{k_2}{k_1}r^2, \qquad \varepsilon_1 \equiv \frac{m_0}{M}, \tag{10}$$

$$\varepsilon_2 \equiv \frac{m_0 r^2}{J + m_0 r^2}, \quad \varepsilon_3 \equiv \frac{m_0 r g M}{k_1(J + m_0 r^2)}, \quad E_1 \equiv \frac{\tilde{E}_1 M}{k_1(J + m_0 r^2)}, \quad E_2 \equiv \frac{\tilde{E}_2 M}{J + m_0 r^2}\sqrt{\frac{M}{k_1}}, \tag{11}$$

$$\gamma \equiv \frac{\xi r}{2\ell}, \quad \sigma \equiv \frac{k_3 M}{k_1 m}. \tag{12}$$

3. Dynamical analysis of the non-ideal system with a liquid damper

The non-ideal system with a liquid damper has the following dynamical variables:

- $(x(t), \dot{x}(t))$: position and velocity of the cart,
- $(y(t), \dot{y}(t))$: position and velocity of the liquid level in the tube,
- $(\varphi(t), \dot{\varphi}(t))$: angular position and angular velocity of the eccentric mass of the rotor.

The combined system phase space has out of 6D, and this is the same dimensionality as of the vector field $\dot{\mathbf{v}} = \mathbf{F}(\mathbf{v})$ corresponding to the governing equations (7)–(9), where $\mathbf{v} = (x, \dot{x}, y, \dot{y}, \varphi, \dot{\varphi})^{\mathrm{T}}$.

The high dimensionality of the phase space and the nonlinearity present in the corresponding vector field limit us almost exclusively to numerical analyses done by integrating the equation set (7)–(9) and examining the dynamical properties of the solutions obtained. In the following we will fix the system parameters as $\mu = 0.01$, $\beta = 0.02$, $\delta = 0.1$, $\varepsilon_1 = 0.1$, $\varepsilon_2 = 0.25$, $\varepsilon_3 = 0$, $E_2 = 1.5$,

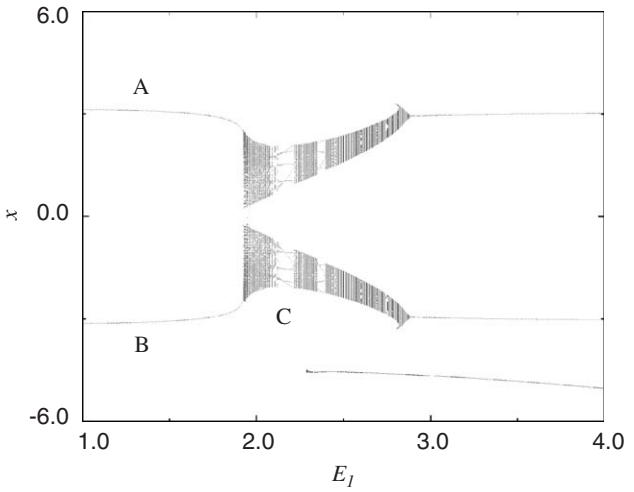

Fig. 2. Bifurcation diagram for the cart position versus the control parameter E_1. The coexisting attractors are labelled A, B, and C.

$\gamma = 0.374656$, and $\sigma = 0.9801$. We will choose, as the control parameters to be studied, the motor constant E_1 and the geometrical aspect ratio α of the liquid damper.

Let us begin by considering the system in absence of a liquid damper, i.e., only the cart motion driven by the unbalanced rotor. Fig. 2 shows the bifurcation diagram for the cart position in terms of the control parameter E_1. For low values of it we have two coexisting limit-cycles (periodic attractors), named as A and B. These attractors suffer an abrupt change at $E_1 \approx 1.9$, where a saddle node bifurcation occurs: the stable orbits A and B collide with unstable orbits (not shown in the bifurcation diagram), and in their place, after the bifurcation, there appears chaotic motion. This is the typical scenario of type-I intermittent transition to chaos [11]. The chaotic region is interspersed with periodic windows, some of them presenting period-doubling bifurcation cascades clearly visible in Fig. 2. Simultaneously, for E_1 greater than ≈ 2.3 there appears a third attractor, named C, which persists for higher E_1 even when the former attractors (A and B) are restored.

The motion of the cart itself can be viewed in a 2D subspace of the full phase space, in which we plot the cart displacement versus velocity. Fig. 3(a) shows phase portraits exhibiting two coexisting limit-cycles A and B. The phase trajectories will asymptote to either one, according to its initial condition. These attractors are located symmetrically with respect to the $x = 0$ and $\dot{x} = 0$ lines, thanks to the $x \to -x$ and $\dot{x} \to -\dot{x}$ symmetries possessed by Eqs. (7)–(9) (only odd powers of x do appear). The gray curves refer to the cart motion without damping by TLCD, whereas black curves include this damping.

Since gray and black curves nearly coincide in Fig. 3(a), we conclude that, at least in this case, the damping effect is practically not noticeable, as can be confirmed by 3(b), where the time series of the cart position are plotted, showing motions of very similar amplitude and frequency. Figs. 3(c) and (d) show the Lyapunov spectrum of coefficients related to the system without control and with a TLCD, respectively. In the latter case there are six coefficients because of the

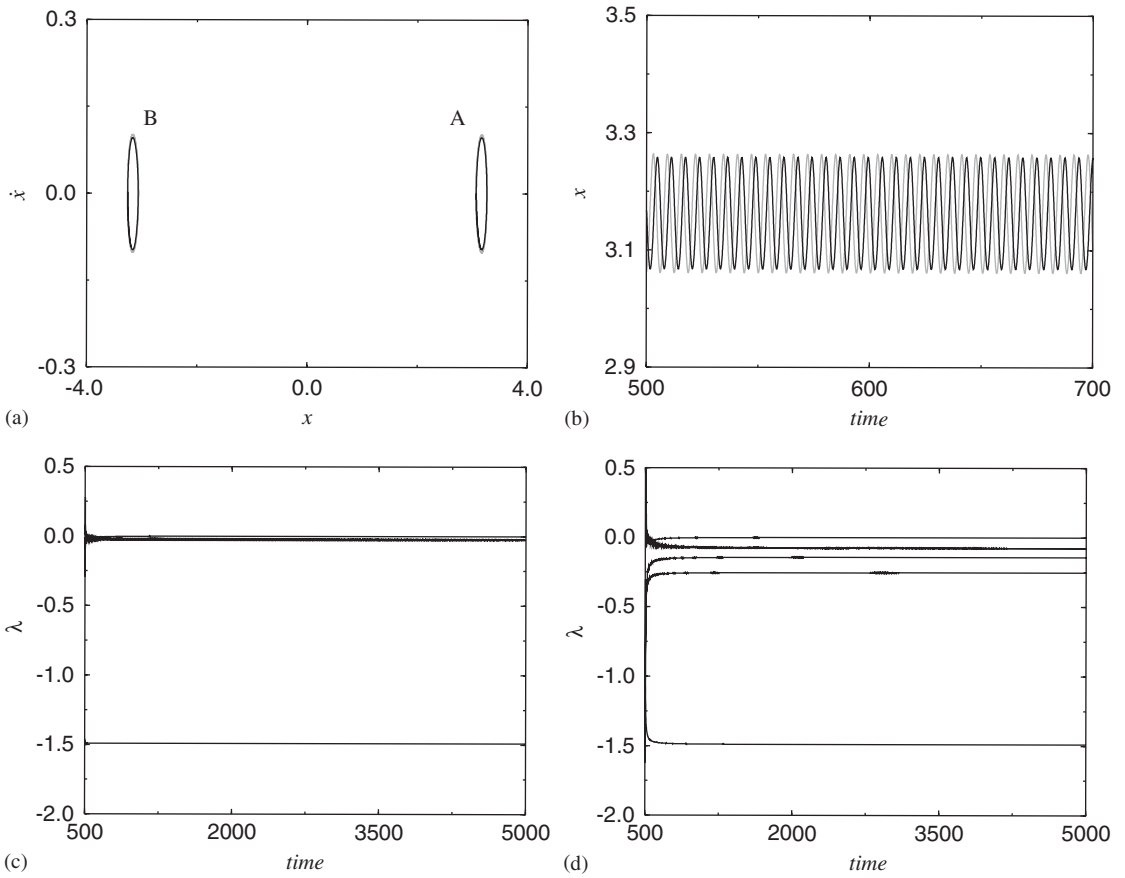

Fig. 3. (a) Displacement versus velocity of the cart, for $E_1 = 1.5$ showing two periodic attractors named as A and B. Gray curves: without TLCD; black curves: with TLCD; (b) time series of the cart displacement for the attractor A with and without TLCD; (c) Lyapunov spectrum without TLCD; (d) with TLCD.

increased phase space dimensionality. As expected, in both cases, all Lyapunov exponents are negative, indicating purely regular motion in all phase space directions. The stationary values of all Lyapunov exponents are found in Table 1.

Fig. 4 shows the basins of attraction corresponding to the attractors A and B of Fig. 3(a), represented as black and white regions, respectively. These regions show up as smooth lobes from which emanate striations which encircle the lobes. The uncontrolled and controlled cases are depicted in Fig. 4(a) and (b), respectively. Both figures are similar to the basin boundary structure displayed by a particle in a two-well potential [12]. In fact, the symmetry of the vector field with respect to $x = 0$ is shared by both systems. Moreover, the motion of the cart itself is essentially of a damped driven Duffing oscillator, thanks to the nonlinear stiffness adopted. It is apparent that the basin filaments are wider in the controlled case, which indicates that, at least for that part of phase space considered, the effect of a TLCD is to decrease the complexity of the basin structure.

As we anticipated in Fig. 2, for higher values of the control parameter E_1 it is possible to observe chaotic dynamics in the system. Fig. 5(a) shows, in the $x \times \dot{x}$ projection of the phase

Table 1
Lyapunov spectrum

$E_1 = 1.5$, no TLCD	$E_1 = 1.5$, with TLCD	$E_1 = 2.0$, no TLCD	$E_1 = 2.0$, with TLCD	$E_1 = 2.5$, no TLCD	$E_1 = 2.5$, with TLCD
0.0000	0.0000	0.0540	−0.0027	0.0004	−0.0037
−0.0241	−0.0767	−0.0003	−0.1264	0.0000	−0.0451
−0.0238	−0.0769	−0.1576	−0.1265	−0.0174	−0.0452
−1.4908	−0.1425	−1.4352	−0.5286	−1.5218	−0.6358
	−0.2535		−0.5285		−0.6957
	−1.4903		−1.4359		−1.5737

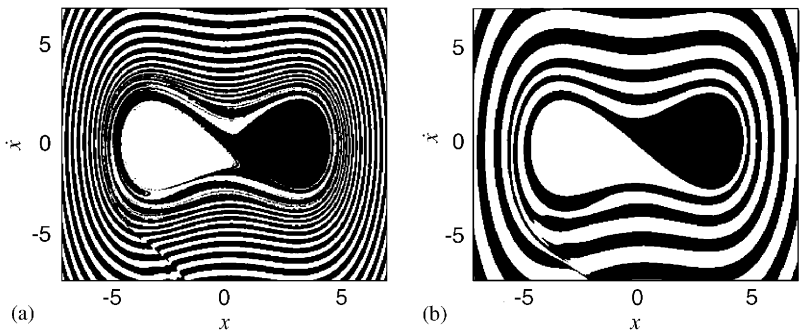

Fig. 4. Basins of attraction of the attractors A (black) and B (white). (a) Without a TLCD ($\alpha = 0$); (b) with a TLCD ($\alpha = 3.0$).

space, two coexisting chaotic attractors (in gray) for the uncontrolled system, named A and B. In this case, the effect of the TLCD is to suppress chaos, since the same attractors, with control, reduce to limit-cycles (in black). Moreover, the amplitude of the periodic oscillations (with TLCD) is roughly one-third of that for uncontrolled chaotic oscillations (Fig. 5(b)). The chaoticity of the attractors without TLCD can be also related to the existence of one positive Lyapunov exponent (Fig. 5(c)); whereas with TLCD all exponents are negative (Fig. 5(d)). The values of these exponents can also be found in Table 1.

Unlike the smooth basin boundary structure typically displayed by periodic attractors like those depicted in Fig. 3, the structure for coexisting chaotic attractors is more involved (Fig. 6(a)). The overall structure is the same, but there are incursive fingers in the lobe filamentation for both basins, and which appear due to homoclinic and heteroclinic crossings between stable and unstable manifolds of periodic orbits (saddle points) belonging to the basin boundaries. In fact, the boundary itself is the closure of the stable manifold of a saddle point belonging to the boundary. Since the unstable manifold of this saddle intercepts both basins (a fact not shown explicitly in Fig. 6(a)), the basin boundary is a fractal curve, with a non-integer box-counting dimension [13,14]. The fractal nature of the boundaries can also be appreciated in Fig. 6(b), where a magnification of a part of the basin structure is shown, revealing the wiggles characteristic of manifold crossings.

However, as we apply the perturbation of a TLCD on the system, besides the high-amplitude chaotic attractors have reduced to low-amplitude limit-cycles, the corresponding basin structure

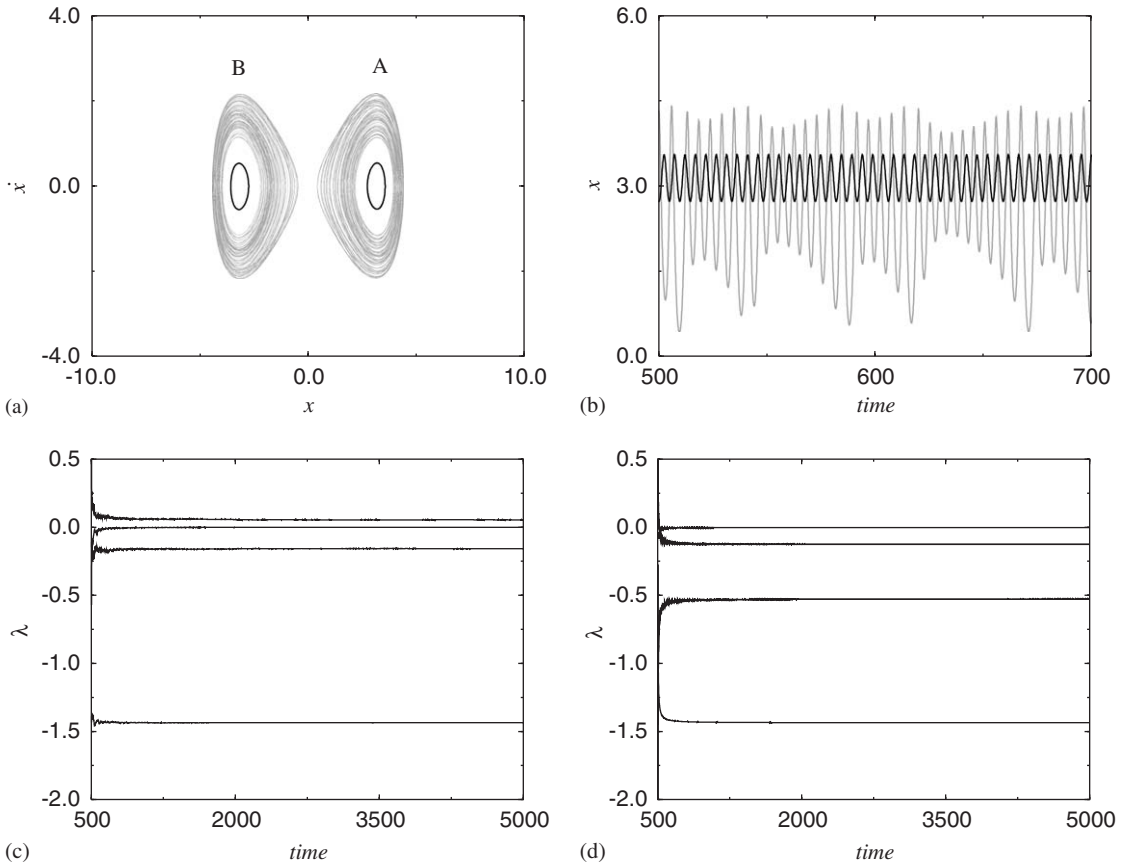

Fig. 5. (a) Displacement versus velocity of the cart, for $E_1 = 2.0$ showing two coexisting attractors named as A and B. Gray curves: chaotic attractors without TLCD; black curves: limit-cycles with TLCD; (b) time series of the cart displacement for the attractor A with and without TLCD; (c) Lyapunov spectrum without TLCD; (d) with TLCD.

has become also less involved (Fig. 6(c), consisting of smooth filaments emanating from the two lobes (see Fig. 6(d) for a magnification).

Up to now we have fixed the geometric ratio of the liquid damper (α) and varied the driving parameter E_1. We can also hold the latter at a constant value, say, $E_1 = 2.0$, and analyze how the cart position changes with the TLCD parameter α. Our results are shown in Fig. 7, where we plot the corresponding bifurcation diagram. Without a liquid damper ($\alpha = 0$) the system will undergo chaotic motion, as already observed. Varying the geometrical ratio of the TLCD this chaotic motion suffers a complicated transition to periodic dynamics for α greater than 2.0.

To conclude this numerical investigation, we can also explore the control parameter E_1-range for which, as shown by Fig. 2, there is a periodic attractor coexisting with two quasi-periodic attractors, as for $E_1 = 2.5$ (Fig. 8(a)). With the liquid damper, the quasi-periodic attractors transform to limit-cycles as before, but the periodic attractor (C) disappears at all (Fig. 8(b)). These conclusions can also be inferred from the Lyapunov spectra (Fig. 8(c) and (d); and Table 1).

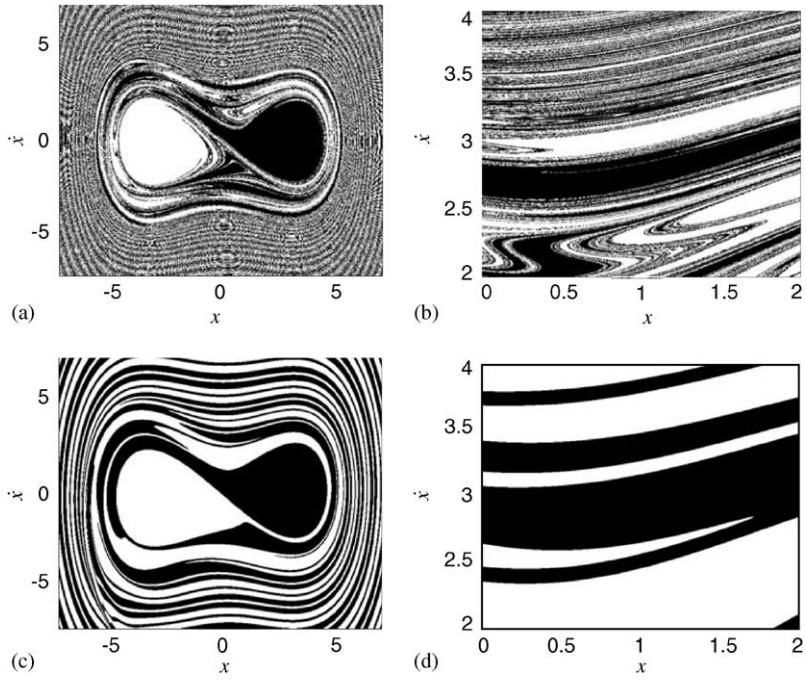

Fig. 6. (a) Basins of attraction of the attractors A (black) and B (white) without a TLCD ($\alpha = 0$); (b) magnification of part of previous figure; (c) basins for the system with a TLCD ($\alpha = 3.0$); (d) magnification of part of previous figure.

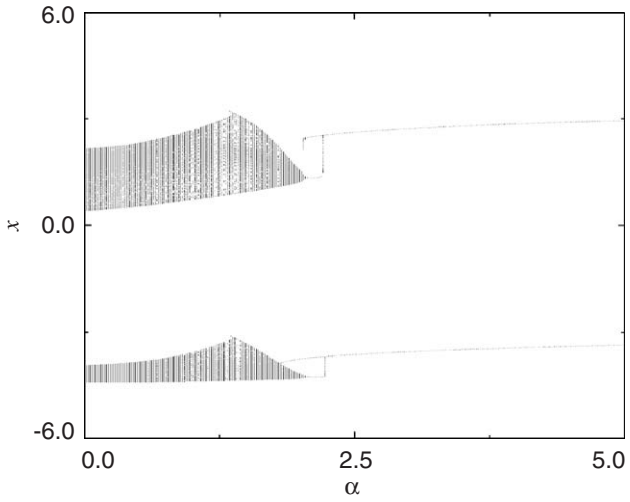

Fig. 7. Bifurcation diagram for the cart position versus the TLCD parameter α.

The structure of the attraction basins is even more involved with three coexisting attractors, as illustrated by Fig. 9(a). In this case, the filamentation of the two main basins (of A and B) are not only interspersed but are also intertwined with the basin of the third attractor (painted in gray). We

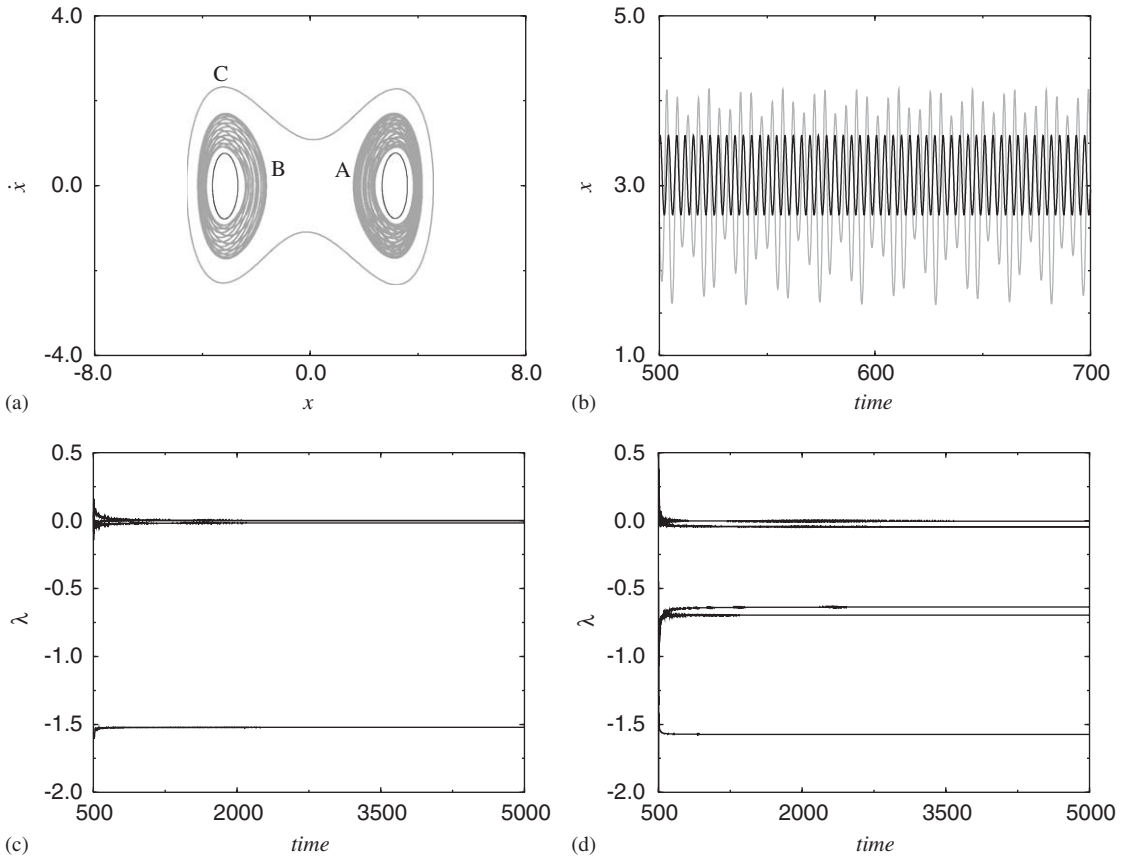

Fig. 8. (a) Displacement versus velocity of the cart, for $E_1 = 2.5$ showing three coexisting attractors named as A, B, and C. Gray curves: quasi-periodic attractors without TLCD; black curves: limit-cycles with TLCD; (b) time series of the cart displacement for the attractor A with and without TLCD; (c) Lyapunov spectrum without TLCD; (d) with TLCD.

conjecture, based on previous results, that the common boundary to all these basins displays not only a fractal nature, but also the stronger Wada property: all boundary points are arbitrarily close to points of all basins, in such a way that a ball centered at any boundary point would intercept all basins of attraction in non-empty sets. The practical consequence of a system having the Wada property is the extreme sensitivity to final state exhibited by such a system: small uncertainties in the determination of the initial condition can lead to complete uncertainty as to what attractor will this initial condition asymptote to. Even with control (Fig. 9(b)) the basin structure will be fractal, although not having the Wada property since the third attractor has disappeared.

4. Conclusions

For the parameter ranges studied in this work we basically conclude that a tuned liquid column damper does not necessarily reduces the amplitude of periodic oscillations. We analyze a situation

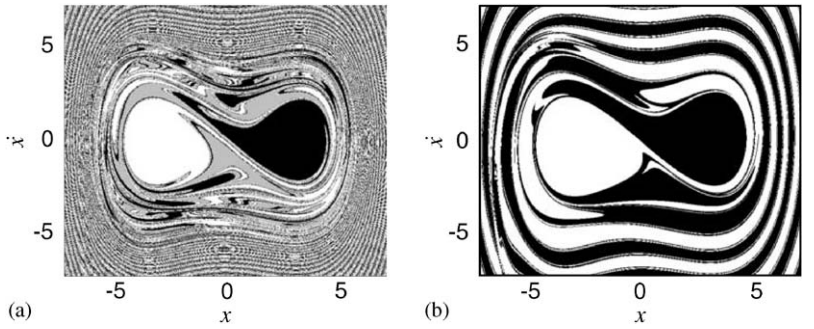

Fig. 9. Basins of attraction of the attractors A (black), B (white), and C (gray) for $E_1 = 2.5$. (a) Without a TLCD ($\alpha = 0$); (b) with a TLCD ($\alpha = 3.0$).

where there are two coexisting limit-cycles and found that the damper effect is almost negligible. On the other hand, when chaotic oscillations are displayed by the vibrating system, the effectiveness of liquid dampers have been demonstrated by (i) the suppression of chaotic motion into a limit-cycle; (ii) a substantial reduction (by a factor of about one-third) of the oscillation amplitudes. Parameter ranges were also found for which there is a third periodic attractor for the uncontrolled system. In this case, the effect of the liquid damper was to suppress this third attractor.

Another result which we obtain is that a liquid damper makes the basin structure simpler in terms of its topological properties. When there are two periodic attractors, the corresponding basins having a smooth boundary, the damper effect is to enlarge the basin filaments. For two chaotic attractors, where the phase space has a convoluted structure (fractal) of basin filaments, the effect of the liquid damper was to make the basin boundary smoother. Finally, when three attractors coexist, the uncontrolled system has a very complicated basin boundary structure, which we conjecture may exhibit the strong topological Wada property, which implies almost complete uncertainty about the final state. The addition of a perturbation by a liquid damper decreases the complexity of the basin structure by washing this latter Wada property.

In all cases studied in this paper, the effectiveness of a TLCD in a vibration structure driven by a limited power source cannot be assured a priori thanks to the complicated dynamical aspects of its behavior. In particular, the original claim that a liquid damper can reduce the amplitude of any oscillation needs to be taken with due caution, and a further dynamical investigation is mandatory. Furthermore, for the considered parameters, a preliminary analysis indicates that the addition of small amounts of noise to non-ideal oscillators with a TLCD does not change significantly their dynamical properties, at least for the parameter ranges considered in this work. For example, we have found that noise perturbations do not typically cause basin hopping, i.e., the alternate switching among different coexisting attractors. Therefore, we expect that noise effect should not alter significantly the action of liquid column dampers on non-ideal oscillators. However, further numerical investigation should be carried to better understand the noise effect in the considered system for other parameter ranges not explored in the present work.

Acknowledgements

This work was made possible by partial financial support from the following Brazilian government agencies: FAPESP, CAPES, CNPq and Fundação Araucária.

References

[1] S. Chaterjee, A.K. Mallik, A. Ghosh, On impact dampers for non-linear vibrating systems, *Journal of Sound and Vibration* 187 (1995) 403–420.
[2] S. Chaterjee, A.K. Mallik, A. Ghosh, Impact dampers for controlling self-excited oscillation, *Journal of Sound and Vibration* 193 (1995) 1003–1014.
[3] J.L.P. Felix, J.M. Balthazar, R.M.L.R.F. Brasil, On tuned liquid column dampers mounted on a structural frame under a non-ideal excitation, *Journal of Sound and Vibration* 282 (2005) 1285–1292.
[4] S.K. Yalla, A. Kareem, Beat phenomenon in combined structure-liquid damper systems, *Engineering Structures* 23 (2001) 622–630.
[5] http://www.nd.edu/~nathaz/research/liquid/liq_damp.html.
[6] V.O. Kononenko, *Vibrating Systems with a Limited Power Supply*, Iliffe Books, London, 1969.
[7] T.S. Krasnopolskaya, A.Y. Shvets, Chaos in vibrating systems with a limited power-supply, *Chaos* 3 (1993) 387–395.
[8] J. Warminsky, J.M. Balthazar, R.M.L.R.F. Brasil, Vibrations of a non-ideal parametrically and self-excited model, *Journal of Sound and Vibration* 245 (2001) 363–374.
[9] S.L.T. de Souza, I.L. Caldas, R.L. Viana, J.M. Balthazar, R.M.L.R.F. Brasil, Impact dampers for controlling chaos in systems with limited power supply, *Journal of Sound and Vibration* 279 (2005) 955–967.
[10] S.L.T. de Souza, I.L. Caldas, J.M. Balthazar, R.M.L.R.F. Brasil, Analysis of regular and irregular dynamics of a non-ideal gear rattling problem, *Journal of the Brazilian Society of Mechanical Sciences* 24 (2002) 111–114.
[11] T. Kapitaniak, *Chaos for Engineers*, Springer, New York, 2000.
[12] F.C. Moon, G.-X. Li, Fractal basin boundaries and homoclinic orbits for periodic motion in a two-well potential, *Physical Review Letters* 55 (1985) 1439–1442.
[13] S.W. McDonald, C. Grebogi, E. Ott, Fractal basin boundaries, *Physica D* 17 (1985) 125–153.
[14] S.W. McDonald, C. Grebogi, E. Ott, Final state sensitivity: an obstruction to predictability, *Physics Letters A* 99 (1983) 415–418.